

## A Density Functional Theory Study of Ground and Low-Lying Excited Electronic States in Defective Graphenes

Hiroto Tachikawa,\* Yoshinori Nagoya, and Hiroshi Kawabata

*Division of Materials Chemistry, Graduate School of Engineering, Hokkaido University, Sapporo 060-8628, Japan*

Received March 30, 2009

**Abstract:** Electronic states of graphenes, whose carbon atoms are terminated by hydrogen atoms (hydrogenated graphene, denoted H-graphene) and defective graphene (one carbon atom was removed from H-graphene, denoted D-graphene) have been investigated by density functional theory. The sizes of graphenes examined in the present study were  $n = 7, 14, 19, 29, 37, 44$ , and 52; where  $n$  is the number of benzene rings in the graphene. The excitation energies of H-graphenes were gradually decreased as a function of the number of rings. In D-graphene, new energy levels for the first and second excited states appeared as low-lying excited states. It was found that the formation of defect sites in graphene produces large decreases in the excitation energies for third and higher excited states. The highest occupied molecular orbital and lowest unoccupied molecular orbital (LUMO) in H-graphene were widely delocalized over the graphene surface. On the other hand, LUMO in D-graphene was localized only in the defect sites. The effects of vacancy defects on both the ground and excited electronic states of graphene were discussed on the basis of theoretical results.

### 1. Introduction

Graphene is a single layer composed of a carbon backbone with a benzene ring structure. An ideal graphene is a semimetal or zero-energy gap semiconductor. It is expected that the graphene can be applied to an electronic device and circuit because it shows electronic conductivity that is higher than that of three-dimensional silicon.<sup>1–3</sup> Experimental results from transport measurements show that graphene has a remarkably high electron mobility at room temperature, with reported values in excess of  $1.5 \times 10^4 - 2.0 \times 10^5$  cm<sup>2</sup>/(V s).<sup>4–6</sup> In addition, the symmetry of the experimentally measured conductance indicates that the mobilities for holes and electrons are nearly the same. The mobility is nearly independent of temperature between 10 and 100 K.<sup>7–9</sup>

Existence of defect vacancy in graphene and carbon nanotube has been pointed out by several groups.<sup>10–22</sup> Acid treatment is known to create defects in carbon materials.<sup>13–15</sup> The C–C bond cleavage is caused by electrophilic attack.

Coleman et al. artificially made the defect in graphene by acid treatment.<sup>19</sup> They treated the graphene surface by using nonoxidizing acid (HCl) and found the carbon vacancy defect with an in-plane orbital. They also carried out band calculations for two vacancy sites and showed that the band gap in defect site is significantly small.

The electronic states of defect in the graphene have been investigated from a theoretical point of view. Yazyev and Helm investigated the magnetism in graphene induced by single carbon atom defects.<sup>11,21</sup> They considered two types of defects, i.e., the hydrogen chemisorption defect and the vacancy defect. The magnetism due to the defect-induced extended states has been found. Using first-principles calculation, Duplock et al. investigated the adsorption of atomic hydrogen on the defect of graphene. They found that a new energy gap was opened due to one of the electronic density of states.<sup>22</sup> Thus, the electronic states of the defect of graphene at the ground state were well understood theoretically. However, electronic states at both ground and excited states of defective graphene are scarcely known.

\* Corresponding author. Fax: 81-11-706-7897. E-mail: hiroto@eng.hokudai.ac.jp

In the present study, ground and low-lying excited states of normal and defective (one carbon atom is removed from the normal graphene) graphene have been investigated by means of density functional theory (DFT) method<sup>23–26</sup> to elucidate the effect of the defect on the electronic states of graphene. In particular, we focus our attention on the excited states of vacancy defect in graphenes.

The article is organized as follows. In the Computational Details Section, we present the structural models of nanographenes, the method used in the geometry optimization, and the electronic structure calculations of graphenes. Results are described in the Results Section. Finally, the Discussion Section gives the model of the electronic excitation of defective graphene, and our conclusions are presented in the Conclusion Section.

## 2. Computational Details

In the present study, normal graphene (denoted by H-graphene) and defective graphene (D-graphene) were examined to elucidate the effect of vacancy defect on the electronic states of graphene. The edges of graphenes were terminated by hydrogen atoms. The defective graphene was made by removing one carbon atom from the graphene. Namely, D-graphene has a vacancy defect in the central region of the graphene. Seven graphenes,  $n = 7, 14, 19, 29, 37, 44$ , and 52, were examined as models of graphene; where  $n$  is the number of benzene rings in graphene. The structures of all graphenes are given in the Supporting Information. The closed-shell singlet states were examined in the present work.

The structures of the graphenes were optimized at the B3LYP/6-31G(d) level of theory. The excitation energies of H-graphene and D-graphene were calculated at the time-dependent (TD)-DFT, B3LYP/6-31G(d) level. In addition, the PW91PW91/3-21G(d) method was used for comparison. To check the basis set and method dependency, the electronic states were calculated by means of the PW91PW91 level for  $n = 7–52$  and the B3LYP/6-311G(d) level for  $n = 7–19$ . Similar results were obtained, suggesting that one can discuss the qualitative feature of electronic states of graphene using the B3LYP/6-31G(d) level. All DFT calculations were carried out using the Gaussian 03 program package.<sup>27</sup>

To check the validity of the B3LYP/6-31G(d) surface, the B3LYP/6-311G(d) calculations were carried out for the defective graphene with  $n = 37$ . The special distributions of molecular orbitals (MOs) around the highest occupied molecular orbital (HOMO) and the lowest unoccupied molecular orbital (LUMO) obtained by the B3LYP/6-311G(d) level were found to be significantly close to those of the B3LYP/6-31G(d) calculations (see Supporting Information). Therefore, the B3LYP/6-31G(d) level of theory is judged to be effective to obtain qualitative features of the present system.

## 3. Results

### 3.1. Electronic States of Hydrogen Terminated Graphene (H-graphene).

The structures of the hydrogen terminated graphene (denoted H-graphene) used in the present study were fully optimized at the B3LYP/6-31G(d) level. For

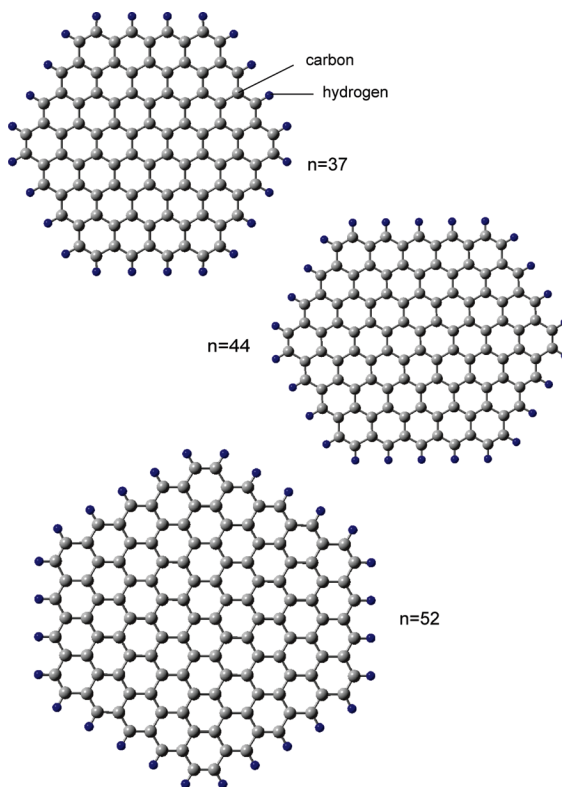


**Figure 1.** Optimized structure of graphenes (H-graphene) obtained by at the B3LYP/6-31G(d) level. Only graphenes with  $n = 37, 44$ , and 52 are given. Edge region of graphene is terminated by hydrogen atoms.

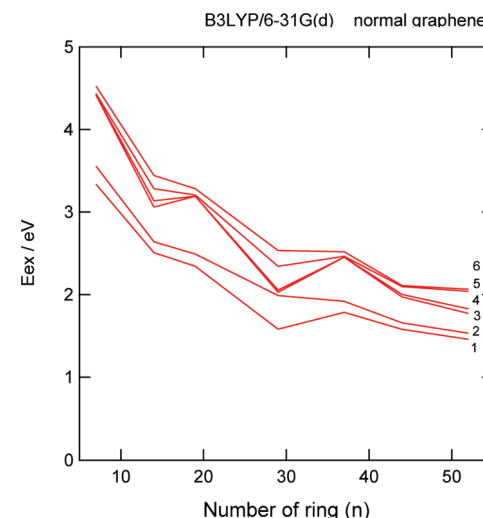


**Figure 2.** Excitation energies of H-graphenes plotted as a function of the size of graphene ( $n$ ). The energies are calculated at the TD-B3LYP/6-31G(d) level. Six electronic excited states are solved.

example, three optimized structures of  $n = 37, 44$ , and 52 are given in Figure 1.

The excitation energies of H-graphenes were calculated as a function of size ( $n$ ) at the TD-B3LYP/6-31G(d) level. The results are given in Figure 2. The excitation energies of  $n = 7$  (smallest size) were calculated to be 3.34 (1st), 3.56 (2nd), and 4.42 eV (3rd excitation energy). It was found that the excitation energy decreases with increasing  $n$ ; for example, the first excitation energies for  $n = 14, 19, 37$ ,

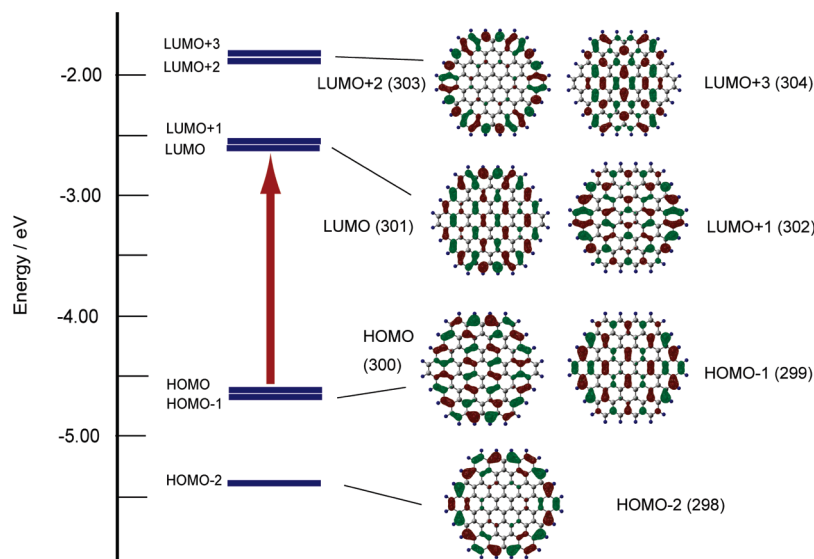


**Figure 3.** MO energies of H-graphenes calculated at the B3LYP/6-31G(d) level. Isosurface indicates special distributions of the molecular orbitals of H-graphene. Arrow indicates main configuration of the first electronic excitations. Orbital numbers are given in parentheses.

**Table 1.** Excitation Energies and Configuration State Functions of H-graphene ( $n = 37$ ) Calculated at the TD-DFT(B3LYP)/6-31G(d) Level

state	CSF and CI vectors	$E_{\text{ex}}$ , eV
$S_1$	$0.515\phi(\text{HOMO-1} \rightarrow \text{LUMO}) - 0.515\phi(\text{HOMO} \rightarrow \text{LUMO+1})$	1.67
$S_2$	$0.492\phi(\text{HOMO-1} \rightarrow \text{LUMO+1}) - 0.492\phi(\text{HOMO} \rightarrow \text{LUMO})$	1.81
$S_3$	$0.331\phi(\text{HOMO} \rightarrow \text{LUMO+4}) - 0.331\phi(\text{HOMO-1} \rightarrow \text{LUMO+3})$	2.34
$S_4$	$0.371\phi(\text{HOMO} \rightarrow \text{LUMO+3}) + 0.331\phi(\text{HOMO-1} \rightarrow \text{LUMO+4})$	2.37

and 52 were calculated to be 2.51, 2.34, 1.69, and 1.46 eV, respectively. The shape of energy curve indicates that the energy gap decreases gradually with increasing  $n$ , and it is almost saturated around  $n = 29$ –52.

The MOs of H-graphene ( $n = 37$ , for example) are illustrated in Figure 3 together with the orbital energies around HOMO and LUMO calculated at the B3LYP/6-31G(d) level. Both HOMO and LUMO are doubly degenerated in energy. The orbitals from HOMO-1 and LUMO+1 are widely delocalized over the graphene surface. On the other hand, those of HOMO-2 and LUMO+2 are localized in edge region of graphene surface. In the case of LUMO+3, the orbital is delocalized again on the surface.

To elucidate the electronic states of graphene at the ground and low-lying excited states, MOs and weights of configuration state functions (CSFs) are analyzed in detail. The excitation energies and CSFs are given in Table 1. The main configurations for the first and second excitations are  $\phi(\text{HOMO-1} \rightarrow \text{LUMO})$  and  $\phi(\text{HOMO} \rightarrow \text{LUMO+1})$ , while the coefficients of CSFs are 0.515 and −0.515, respectively. Here,  $\phi(\text{HOMO} \rightarrow \text{LUMO})$  means a CSF where one electron is excited from HOMO to LUMO.

It should be noted that HOMO and HOMO-1 are doubly degenerated, while LUMO and LUMO+1 are also doubly degenerated. These results indicate that the low-lying excited states of graphene are composed of the HOMO–LUMO excitations.

**3.2. Electronic States of D-graphene.** To elucidate the effects of the defect on the electronic states of graphene,

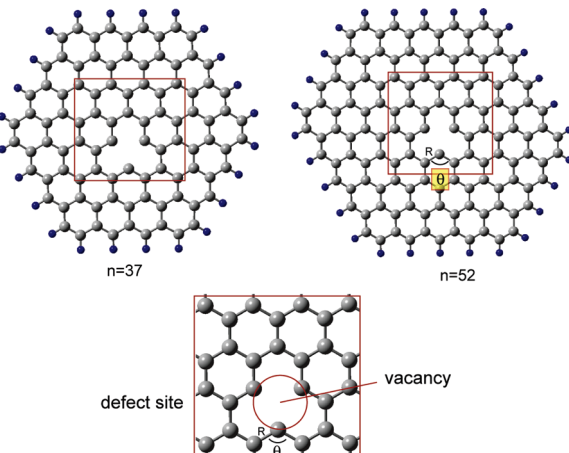


**Figure 4.** Optimized structure of D-graphene obtained by at the B3LYP/6-31G(d) level. Only D-graphenes with  $n = 37$ , 44, and 52 are given. Edge region of graphene is terminated by hydrogen atoms.

a defect was artificially made on the graphene. The defect is made by removing one carbon atom located around the center of H-graphene. The geometry of each D-graphene was optimized at the B3LYP/6-31G(d) level. The structures of the D-graphenes for  $n = 37$  and 52 are illustrated in Figure 4.

The stabilization energy obtained by the geometry optimization was calculated to be 14.0 kcal/mol ( $n = 37$ ). The C–C bond length (=R) and C–C–C angle (=θ) in the defect site were changed from 1.425 Å and 120.1° to 1.393 Å and 123.8°, respectively. The bond lengths were slightly shortened and the angle is wider by the deformation.

The excitation energies of defective graphenes ( $n = 7$ , 14, 19, 37, 44, and 52) are plotted in Figure 5 as a function of  $n$ . The energy level for  $n = 29$  was not given because the TD calculation was not converged in case of  $n = 29$ . The excitation energy decreased with increasing  $n$  as well as that of H-graphene. It was found that the excitation energies of

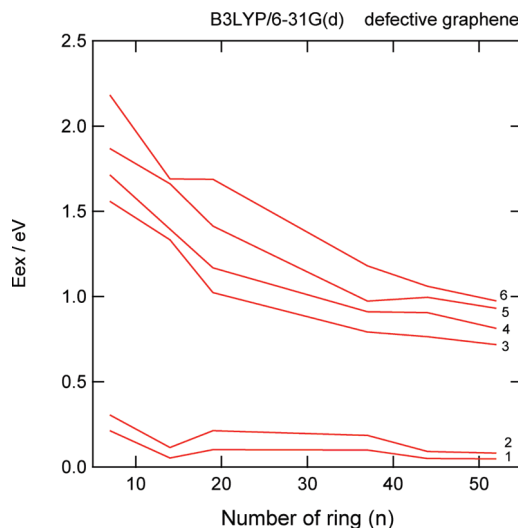


**Figure 5.** Excitation energies of D-graphenes plotted as a function of size of graphene ( $n$ ). The energies are calculated at the TD-B3LYP/6-31G(d) level. Six electronic excited states are solved.

the defective graphene at the first and second excitations were significantly lower than those of H-graphene (below 0.15 eV). Also, it is shown that the first and second excitation energies were not dependent on size ( $n$ ). In contrast, third and higher excitation energies in the defective graphenes were strongly dependent on  $n$ , and these energy levels were also lower than those of H-graphene; for example, the third excitation energy for the defective graphene with  $n = 52$  is 0.72 eV, while that of H-graphene with  $n = 52$  is 1.77 eV.

Thus, it was found that new energy levels (first and second excited states) appear by the formation of a vacancy defect in graphene. The energy levels for the first and second excitations of D-graphenes are significantly lower than those of H-graphenes. These excitations are not dependent on the size of graphene. On the other hand, the third and higher

**Table 2.** Excitation Energies and Configuration State Functions of D-graphene ( $n = 37$ ) Calculated at the TD-DFT(B3LYP)/6-31G(d) Level

state	CSF and CI vectors	$E_{ex}$ , eV
$S_1$	$0.614\phi(\text{HOMO} \rightarrow \text{LUMO}) - 0.126\phi(\text{HOMO-2} \rightarrow \text{LUMO})$	0.405
$S_2$	$0.631\phi(\text{HOMO} \rightarrow \text{LUMO+1}) - 0.156\phi(\text{HOMO-2} \rightarrow \text{LUMO+1})$	0.468
$S_3$	$0.694\phi(\text{HOMO-1} \rightarrow \text{LUMO})$	1.035
$S_4$	$0.696\phi(\text{HOMO-1} \rightarrow \text{LUMO+1})$	1.067

excitation energies are strongly dependent on cluster size ( $n$ ). The lower energy levels obtained in the D-graphene are much different from that of H-graphenes.

To elucidate the specific electronic feature in D-graphene, molecular orbitals (MOs) and weights of configuration state functions (CSFs) at the excited states are analyzed in detail. The special distributions of MOs and orbital energies around HOMO and LUMO are given in Figure 6. It was found that HOMO, HOMO-1, and HOMO-2 are widely delocalized on graphene surface. On the other hand, LUMO and LUMO+1 are localized in the defect site. This feature is much different from the H-graphene in which both HOMO and LUMO are delocalized on the graphene surface. These results indicate that formation of vacancy defect causes a large change of electronic states of graphene. Especially, it can be expected that the excited and anionic states of graphene are strongly affected by the defect.

The coefficients of CSFs in the D-graphene are summarized in Table 2. The first excited state was mainly composed of two CSFs,  $\phi(\text{HOMO} \rightarrow \text{LUMO+1})$  and  $\phi(\text{HOMO-2} \rightarrow \text{LUMO})$ , while the coefficients of CSFs for the former and the latter were calculated to be 0.914 and -0.126, respectively. The second excited state is mainly composed of  $\phi(\text{HOMO} \rightarrow \text{LUMO+1})$  with the coefficient of 0.631. The first and second excitations are almost degenerated in from energy each other. Therefore, the first excitation band ( $S_0 \rightarrow S_1$  and  $S_0 \rightarrow S_2$ ) can be assigned to a charge transfer (CT) band from the bulk surface to the defect

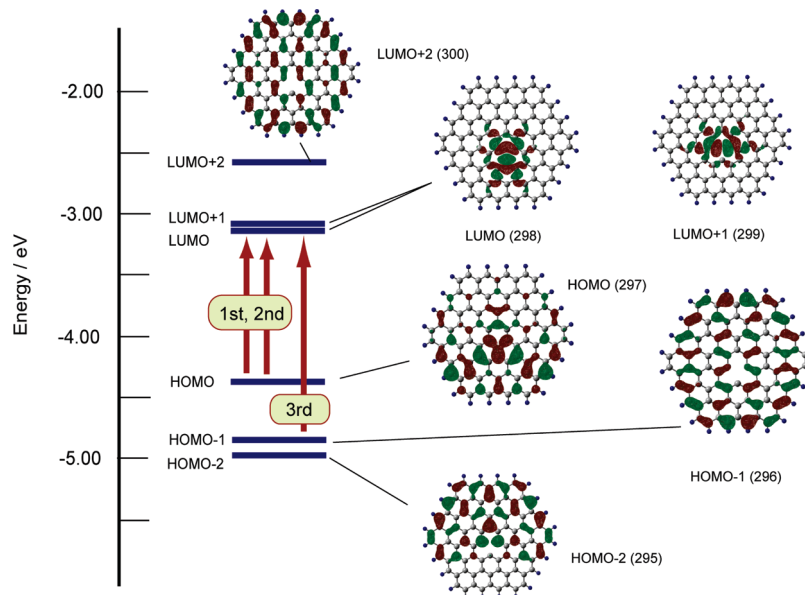


**Figure 6.** Molecular orbital energies of D-graphenes calculated at the B3LYP/6-31G(d) level. Isosurface indicates the special distributions of molecular orbitals of D-graphene. Arrows indicate main configurations of first, second, and third electronic excitations. Orbital numbers are given in parentheses.

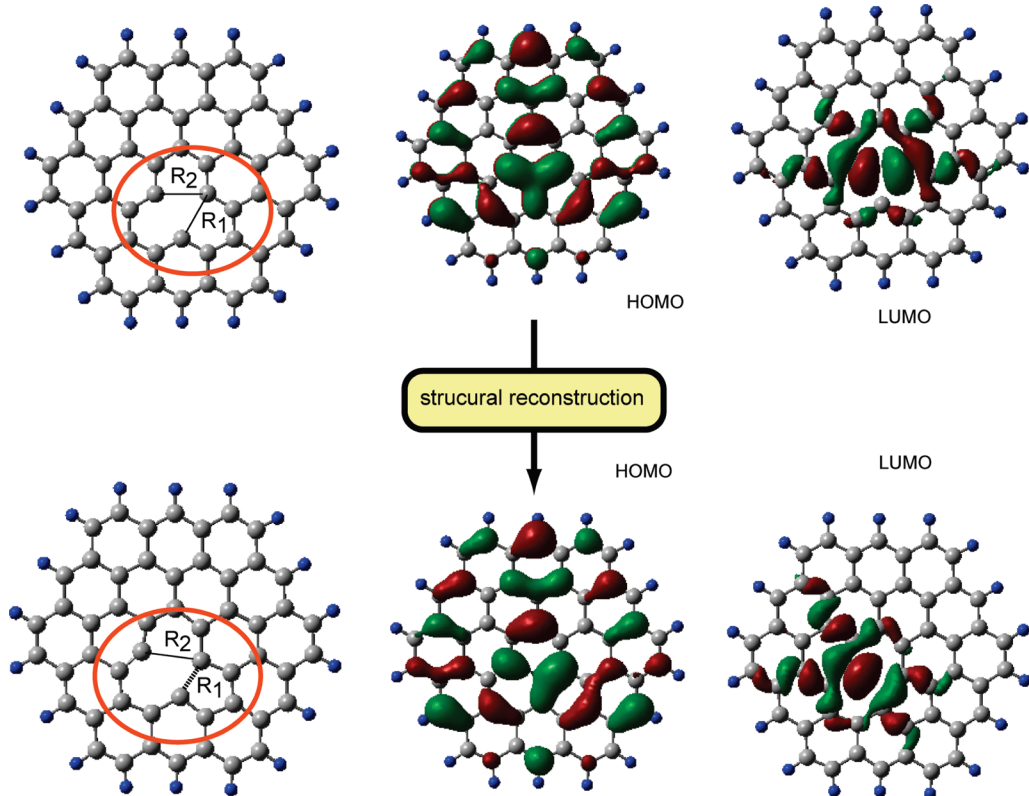


**Figure 7.** Special distributions of HOMO and LUMO of D-graphenes before and after structural reconstruction.

site. The third and forth excitation bands are also attributed to one of the CT bands.

**3.3. Effects of Structural Reconstruction of D-graphene on the Electronic States.** It is known that a vacancy defect undergoes reconstruction by thermal activation. In this section, the effects of reconstruction on the excitation energies are discussed. The optimized structures of D-graphene ( $n = 19$ ) before and after structural reconstruction are illustrated in Figure 7. The large vacancy with three benzene rings is formed before structural reconstruction. The bond distances between carbon atoms are  $R_1 = 2.433 \text{ \AA}$  and  $R_2 = 2.463 \text{ \AA}$ . After the reconstruction, the bond distances are changed to  $R_1 = 1.866 \text{ \AA}$  and  $R_2 = 2.694 \text{ \AA}$ , indicating that the one of the C–C bonds is significantly shortened and a new C–C bond is formed by the reconstruction. The stabilization energy is 14.4 kcal/mol at the B3LYP/6-31G(d) level. However, distributions of HOMO and LUMO show that the shapes of orbitals are not strongly affected by the reconstruction. The excitation energies of D-graphene are calculated to be 0.435 (1st) and 0.566 eV (2nd) before the reconstruction and 0.290 (1st) and 0.470 eV (2nd) after the reconstruction, indicating that the reconstruction affects the excitation energies. However, the assignment of the excitation is not changed.

## 4. Discussion

**4.1. Model of Electronic Excitation in D-graphene.** In the present study, the electronic states of D-graphene have been investigated by means of the DFT method. A single vacancy defect was examined and compared with pure

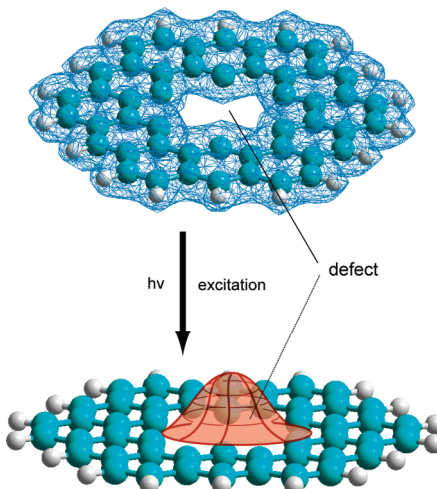


**Figure 8.** Schematic illustration of a model of electronic excitations of D-graphene. The electron is concentrated in the defect site by the electronic excitation.

graphene. It was found that low-lying excited states newly appear by the formation of defect. These excited states are composed of electron transfer bands from the bulk surface to the defect site.

On the basis of the present results, we propose a model for the electronic excitations of D-graphene, which is illustrated schematically in Figure 8. The D-graphene has new energy bands at lower energy levels below 0.15 eV. HOMO of the D-graphene is distributed widely on the graphene surface as shown in Figure 8 (upper). After the electronic excitation of D-graphene, the electron is transferred from the bulk region to the defect site. Namely, it is found

that the D-graphene has a lowest excitation band corresponding to a charge transfer band from the bulk to defect site.

**4.2. Comparison with Previous Studies.** Recently, Coleman et al. investigated experimentally a defect vacancy in a graphene sheet.<sup>19</sup> They treated the graphene sheet with an acid treatment (HCl) and made a vacancy defect in the graphene surface. It was suggested that defect vacancy has a metallic conductivity. The present calculation strongly supports this feature; namely, the band gap of graphene is significantly decreased by the formation of a vacancy defect. The first excitation energy is changed from 1.46 to 0.05 eV by the formation of a vacancy defect ( $n = 52$ ) at the B3LYP/6-31G(d) level.

In the present study, the closed-shell singlet states were discussed only as an electronic structure. However, it has been pointed out that the spin polarization is important in open-shell singlet states of nanosized graphenes.<sup>28</sup> Jiang and Dai investigated that the electronic ground states of acenes with different numbers of fused benzene rings (up to 40 rings) have been studied with first principles spin-polarized DFT. The ground states of higher acenes (>7 rings) are found to be antiferromagnetic (i.e., open-shell singlet). To elucidate the electronic structures of graphenes in details, the calculations of open-shell singlet excited states are needed in the near future. For comparison, the spin density of graphene ( $n = 37$ ) at the triplet states was calculated. The distribution of spin density is illustrated in Supporting Information (Figure S7). The unpaired electrons were mainly localized in the defect site, but the tail of the distribution is widely delocalized over the graphene surface. However, the energy of triplet state was close to that of the singlet ground state (the  $T_1$  state was only 0.3 kcal/mol higher in energy than the  $S_0$  state). Therefore, the investigation of electronic states at the triplet states will be needed in the near future to elucidate the detailed electronic structure of D-graphene.

It has been pointed out that the TD-DFT method without Hartree–Fock (HF) exchange misses completely the excitonic effects. The magnitude of the error would be dependent on the system. There are cases where the error can be quite significant.<sup>29</sup> In the case of a large system, the effects may be large.<sup>30</sup> To validate the TD-DFT(B3LYP) calculations in the present system, time-dependent HF (TDHF) calculations<sup>31,32</sup> have been done for comparison. The results are given in the Supporting Information. The shapes of MOs around the HOMO are in good agreement with the TD-DFT calculations. The excitation energies of D-graphene calculated by TDHF were slightly larger than those of TDDFT. The assignment of electronic excitations is agreement with each other. Therefore, TD-DFT(B3LYP) calculation would give a reasonable electronic structure of the D-graphene in a qualitative feature.

## 5. Conclusion

In the present study, the electronic states of normal and defective graphenes (denoted by H- and D-graphenes, respectively) have been investigated by density functional theory (DFT) calculations. The sizes of graphenes examined in the present study were  $n = 7, 14, 19, 29, 37, 44$ , and 52; where  $n$  is the number of benzene rings in the graphene.

The excitation energies of H-graphenes were gradually decreased as a function of the number of rings. In D-graphene, new energy levels for the first and second excited states appeared as low-lying excited states. The formation of defect sites in graphene produces large decreases in the excitation energies for third and higher excited states. The first excitation band of D-graphene is assigned as a charge transfer band from the bulk to the defect site.

**Acknowledgment.** H.T. is indebted to the Computer Center at the Institute for Molecular Science (IMS) for the use of the computing facilities. He also acknowledges partial support from the Iketani Foundation and a grant-in-aid for Scientific Research (C) from the Japan Society for the Promotion of Science (JSPS). This work was partially supported by the KURATA foundation.

**Supporting Information Available:** Illustrations of optimized structures of D-graphene ( $n = 7, 14, 19, 29, 37, 44$ , and 52), and excitation energies of H- and D-graphenes were calculated at several levels of theory. This material is available free of charge via the Internet at <http://pubs.acs.org>.

## References

- (1) Geim, A. K.; Novoselov, K. S. The rise of graphene. *Nat. Mater.* **2007**, *6*, 183–191.
- (2) Novoselov, K. S. *Nat. Mater.* **2007**, *6*, 720–721.
- (3) Yang, L.; Cohen, M. L.; Louie, S. G. *Phys. Rev. Lett.* **2008**, *101*, 186401.
- (4) Morozov, S. V.; Novoselov, K. S.; Katsnelson, M. I.; Schedin, F.; Elias, D. C.; Jaszczak, J. A.; Geim, A. K. *Phys. Rev. Lett.* **2008**, *100*, 016602.
- (5) Bolotin, K. I.; Sikes, K. J.; Hone, J.; Stormer, H. L.; Kim, P. *Phys. Rev. Lett.* **2008**, *101*, 096802.
- (6) Chen, J.-H.; Jang, C.; Xiao, S.; Ishigami, M.; Fuhrer, M. S. *Nature Nanotechnol.* **2008**, *3*, 206.
- (7) Novoselov, K. S.; Geim, A. K.; Morozov, S. V.; Jiang, D.; Katsnelson, M. I.; Grigorieva, I. V.; Dubonosand, S. V.; Firsov, A. A. *Nature* **2005**, *438*, 197.
- (8) Wehling, T. O.; Novoselov, K. S.; Morozov, S. V.; Vdovin, E. E.; Katsnelson, M. I.; Geim, A. K.; Lichtenstein, A. I. *Nano Lett.* **2008**, *8*, 173–177.
- (9) Hwang, E. H.; Das Sarma, S. *Phys. Rev.* **2009**, *79*, 165404.
- (10) Khare, R.; Mielke, S. L.; Paci, J. T.; Zhang, S.; Ballarini, R.; Schatz, G. C.; Belytschko, T. *Phys. Rev. B: Condens. Matter Mater. Phys.* **2007**, *75*, 075412.
- (11) Yazyev, O. V.; Helm, L. *Phys. Rev. B: Condens. Matter Mater. Phys.* **2007**, *75*, 125408.
- (12) Rocha, A. R.; Padilha, J. E.; Fazzio, A.; da Silva, A. J. R. *Phys. Rev. B: Condens. Matter Mater. Phys.* **2008**, *77*, 153406.
- (13) Li, T. C.; Lu, S.-P. *Phys. Rev. B: Condens. Matter Mater. Phys.* **2007**, *77*, 085408.
- (14) Pimenta, M. A.; Dresselhaus, G.; Dresselhaus, M. S.; Cancado, L. G.; Jorio, A.; Saito, R. *Phys. Chem. Chem. Phys.* **2007**, *9*, 1276–1291.
- (15) Kuemmeth, F.; Ilani, S.; Ralph, D. C.; McEuen, P. L. *Nature* **2008**, *452*, 448–452.

- (16) Balasubramanian, K.; Burghard, M. *Small* **2005**, *1*, 180–192.
- (17) Itkis, M. E.; Perea, D. E.; Jung, R.; Niyogi, S.; Haddon, R. C. *J. Am. Chem. Soc.* **2005**, *127*, 3439–3448.
- (18) Strano, M. S.; Huffman, C. B.; Moore, V. C.; O’Connell, M. J.; Haroz, E. H.; Hubbard, J.; Miller, M.; Rialon, K.; Kittrell, C.; Ramesh, S.; Hauge, R. H.; Smalley, R. E. *J. Phys. Chem. B* **2003**, *107*, 69796985.
- (19) Coleman, V. A.; Knut, R.; Karis, O.; Grennberg, H.; Jansson, U.; Quinlan, R.; Holloway, B. C.; Sanyal, B.; Eriksson, O. *J. Phys. D: Appl. Phys.* **2008**, *41*, 062001.
- (20) Boukhvalov, D. W.; Katsnelson, M. I. *Nano Lett.* **2008**, *8*, 4373–4379.
- (21) Yazyev, O. V.; Helm, L. *J. Phys. Conf. Ser.* **2007**, *61*, 1294–1298.
- (22) Duplock, E. J.; Scheffler, M.; Lindan, P. J. D. *Phys. Rev. Lett.* **2004**, *92*, 225502.
- (23) Tachikawa, H.; Shimizu, A. *J. Phys. Chem. B* **2005**, *109*, 13255–13262.
- (24) Tachikawa, H.; Shimizu, A. *J. Phys. Chem. B* **2006**, *110*, 20445–20450.
- (25) Tachikawa, H. *J. Phys. Chem. C* **2007**, *111*, 13087–13091.
- (26) Tachikawa, H. *J. Phys. Chem. C* **2008**, *112*, 10193–10199.
- (27) Frisch, M. J.; Trucks, G. W.; Schlegel, H. B.; Scuseria, G. E.; Robb, M. A.; Cheeseman, J. R.; Montgomery, J. A., Jr.; Vreven, T.; Kudin, K. N.; Burant, J. C.; Millam, J. M.; Iyengar, S. S.; Tomasi, J.; Barone, V.; Mennucci, B.; Cossi, M.; Scalmani, G.; Rega, N.; Petersson, G. A.; Nakatsuji, H.; Hada, M.; Ehara, M.; Toyota, K.; Fukuda, R.; Hasegawa, J.; Ishida, M.; Nakajima, T.; Honda, Y.; Kitao, O.; Nakai, H.; Klene, M.; Li, X.; Knox, J. E.; Hratchian, H. P.; Cross, J. B.; Bakken, V.; Adamo, C.; Jaramillo, J.; Gomperts, R.; Stratmann, R. E.; Yazyev, O.; Austin, A. J.; Cammi, R.; Pomelli, C.; Ochterski, J. W.; Ayala, P. Y.; Morokuma, K.; Voth, G. A.; Salvador, P.; Dannenberg, J. J.; Zakrzewski, V. G.; Dapprich, S.; Daniels, A. D.; Strain, M. C.; Farkas, O.; Malick, D. K.; Rabuck, A. D.; Raghavachari, K.; Foresman, J. B.; Ortiz, J. V.; Cui, Q.; Baboul, A. G.; Clifford, S.; Cioslowski, J.; Stefanov, B. B.; Liu, G.; Liashenko, A.; Piskorz, P.; Komaromi, I.; Martin, R. L.; Fox, D. J.; Keith, T.; Al-Laham, M. A.; Peng, C. Y.; Nanayakkara, A.; Challacombe, M.; Gill, P. M. W.; Johnson, B.; Chen, W.; Wong, M. W.; Gonzalez, C.; Pople, J. A. *Gaussian 03*, Revision B.04; Gaussian, Inc.: Pittsburgh PA, 2003.
- (28) Jiang, D.; Dai, S. *J. Phys. Chem. A* **2008**, *112*, 332–335.
- (29) Yang, L.; Cohen, M. L.; Louie, S. G. *Nano Lett.* **2007**, *7*, 3112–3115.
- (30) Izmaylov, A. F.; Scuseria, G. E. *J. Chem. Phys.* **2008**, *129*, 034101.
- (31) Hieringer, W.; Gorling, A. *Chem. Phys. Lett.* **2006**, *426*, 234–236.
- (32) Hieringer, W.; Gorling, A. *Chem. Phys. Lett.* **2006**, *419*, 557–562.

CT900151S